


 Cite this: *RSC Adv.*, 2021, **11**, 34263

 Received 7th August 2021  
 Accepted 12th October 2021

 DOI: 10.1039/d1ra05981e  
[rsc.li/rsc-advances](http://rsc.li/rsc-advances)

## Optimization of synthetic parameters of high-purity trifunctional mercaptoesters and their curing behavior for the thiol–epoxy click reaction†

 Seung-Mo Hong, Oh Young Kim and Seok-Ho Hwang \*

The direct esterification reaction between 3-mercaptopropionic acid (3-MPA) and trimethylolpropane (TMP) was conducted in the presence of various catalyst concentrations of *p*-toluenesulfonic acid (*p*-TSA) to examine the optimized synthetic conditions needed to produce high-purity trimethylolpropane-tris(3-mercaptopropionate) (TMPMP). The purity of the desired TMPMP and uncompleted side-product reduced as the acid catalyst concentration in this esterification reaction increased while the generation of thioester-based side-product increased. The equivalent ratio between epoxy and the manufactured TMPMP was maintained at 1:1 to monitor the curing behavior of the thiol–epoxy click reaction using the DSC technique. The thermal features of the base-catalyzed TMPMP-cured epoxy resin were assessed according to the purity of the TMPMP curing agent.

### Introduction

Thiol-based click chemistry is a type of “click chemistry” that is rapidly gaining popularity in organic chemistry and materials science research for achieving synthetic goals ranging from small molecules to crosslinked macromolecular networks.<sup>1</sup> In particular, base-catalyzed thiol–epoxy click polymerization is generally a good example of an exceptional variety of click reaction owing to its advantages, including fast reaction rate, excellent chemoselectivity, mild reaction conditions, and high yields.<sup>2–8</sup> The mechanism of this reaction is in accordance with the anionic nucleophilic attack to a rarely exchanged carbon on an epoxy ring through a thiolate anion.<sup>9</sup> In detail, the thiolate anions induced through the deprotonation of thiols by the acceleration of a base catalyst react with the better electrophilic carbon of the epoxide group to produce a new carbon–sulfur–carbon bond. The amine utilized in this reaction is a real thermal catalyst since it is not absorbed during the ring-opening reaction. This special mechanism reduces the sensitivity of thiol–epoxy polymerization to oxygen and impurities except for acidic compounds. Furthermore, the cured products are characterized by lower shrinkage, better adhesion, and superior chemical resistance.<sup>10</sup> Multifunctional thiol–epoxy composites with outstanding characteristics have recently drawn a lot of interest.<sup>11–15</sup>

*Materials Chemistry & Engineering Laboratory, School of Polymer System Engineering, Dankook University, Yongin, Gyeonggi-do 16890, Republic of Korea. E-mail: bach@dankook.ac.kr*

† Electronic supplementary information (ESI) available: Result plots of preliminary esterification reactions as well as LC/MS, <sup>1</sup>H NMR, and FT-IR spectra of the crude product. See DOI: 10.1039/d1ra05981e

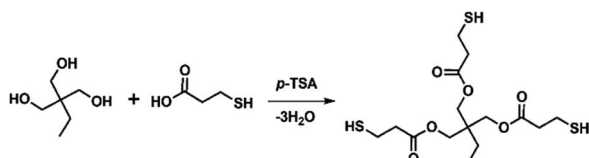
Commercially available multifunctional thiols are limited to a handful of three- and four-armed mercaptoesters despite their potential utility in multifunctional thiol derivatives. Furthermore, a general and efficient synthesis of multi-thiols is unknown, owing to the harsh conditions and several processes necessary to synthesize thiols in general.<sup>16</sup>

The optimal synthesis conditions for producing high-purity three-armed mercaptoesters, trimethylolpropane-tris(3-mercaptopropionate) (TMPMP), are first presented in this study. It is synthesized by reacting ordinal polyhydric alcohol with an ordinal mercaptocarboxylic acid in the presence of a catalytic acid and distilling off the water that is produced as a by-product outside the reaction system. We then describe the thiol-purity reliance on the curing behavior of a diglycidyl ether of bisphenol A (DGEBA) epoxy resin using TMPMP. Their curing behavior, as well as the crosslinked epoxy resins obtained by the base-catalyzed curing reaction, were characterized using calorimetry and thermogravimetry.

### Results and discussion

Trimethylolpropane-tris(3-mercaptopropionate) (TMPMP) is fairly common commercial chemical. To the best of our knowledge, the commercialized TMPMP has quietly low purity, which are made up of the desired product (TMPMP) and by-products produced by an uncompleted esterification reaction as well as a direct thioesterification from a carboxylic acid and thiol.<sup>17</sup> From the atom-economical<sup>18</sup> and environmental points perspective, the optimized synthetic condition is necessary to obtain a desired product with high-purity (Scheme 1). As a result, we utilized LC-MS chromatographic technique to characterization the commercialized TMPMP sample and





Scheme 1 Synthetic route for trimethylolpropane-tris(3-mercaptopropionate) (TMPMP).

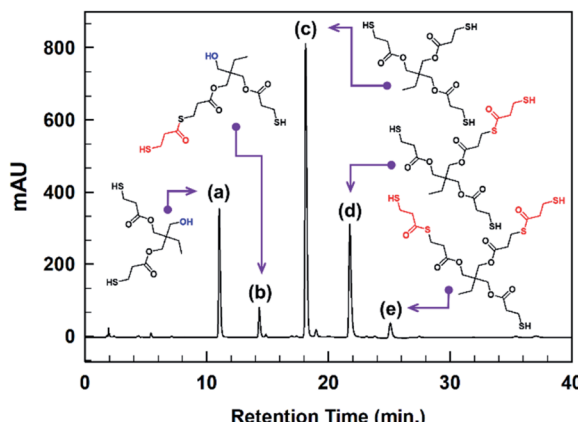


Fig. 1 HPLC chromatogram of a commercialized TMPMP sample and the expected structures of each eluted peak analyzed through mass technique (see; each chemical names in ESI: Table S1†).

examine what kinds of impurities it contains. Potential impurities were identified by comparing its retention times and LC-MS with ESI analysis was used to confirm them further (ESI: Fig. S1†).

The chromatogram of the commercialized TMPMP sample solution and the expected chemical structures for each eluted peak are indicated in Fig. 1.

As indicated in Fig. S1,† the desired product eluted at RT of 14.5 min showed  $m/z$  421  $[M + Na]^+$  in positive ion mode, which was the sodium adduct of the desired TMPMP. Based on the MS technique, the impurities were analyzed as two categories for side-products, which are uncompleted side-products containing unreacted hydroxyl group of TMP and side-products included in the thioester linkage. Although there are various synthetic parameters in the direct esterification reaction, the

reactant mole ratio and catalyst concentration can be regulated directly. Therefore, according to the design of the experiment (DOE), we selected two parameters, including reactant mole ratio and catalyst concentration, to influence the high conversion of desired products. Also, the side-product [ $Y_1 = (a) + (b)$  peak area] containing unreacted hydroxy group and the other side-product [ $Y_2 = (b) + (d) + (e)$  peak area] produced by thio-esterification reaction as the characteristic values were selected. Here  $Y_2$  side-product is more desired than  $Y_1$  side-product because  $Y_2$  is tri-functional mercaptoester, whereas  $Y_1$  is only di-functional mercaptoester.

Preliminary (screening) esterification reaction experiments (Table 1) were conducted to identify the suitable synthetic parameters and their levels in simple azeotropic reflux conditions. In this study, since the purity comparison for these reaction crude products was so tough using  $^1\text{H-NMR}$  and FT-IR (ESI: Fig. S2 and S3†), the chromatography method was applied. Fig. 2 demonstrated the chromatograms of the crude product samples after preliminary reaction and their peak area integrals were also tabulated in Table 1. In all cases, the desired product peak and the distinct four side-product peaks came out just as the chromatogram of the commercialized TMPMP sample. The conversion of desired TMPMP product (c) was in the range of 52.4% to 69.4%. Based on these preliminary experiments, analysis of the effect of main factors and interactions on the conversion of side-products,  $Y_1$  and  $Y_2$ , were plotted as shown in Fig. S4 (ESI†). These plots are according to the data given in Table 1. As shown in Fig. S4,† it was found that the  $Y_2$  value increased and  $Y_1$  value decreased remarkably with increasing catalyst concentration, whereas their trend was stagnated with increase reactant, 3-MPA, concentration. As a result, out of the two parameters used in this study, the dominant factor for the synthesis of TMPMP was the acid catalyst concentration.

To elucidate the role of the catalyst concentration in this study, the various catalyst concentrations from 0.01 to 0.10 mol  $\text{mol}^{-1}$  of a TMP (Table 2) were designed and examined from the composition of the uncompleted side-products ( $Y_1$ ) and thioester-based side-products ( $Y_2$ ) under simple azeotropic reflux condition. The chromatograms for this reaction (entry EXP-1-EXP-5) mixtures are presented in Fig. 3 and their peak area integrals are summarized in Table 2. The conversion of the desired TMPMP was governed by the catalyst concentration. Fig. 4 indicates the influence of the catalyst concentration ranging from 0.01 to 0.10 mol  $\text{mol}^{-1}$  of a TMP on the conversion

Table 1 The composition of the direct esterification of the preliminary reaction and the summary of chromatographic analysis data after the reaction

Entry	Reactant composition (mole)			Peak area integral (%)					Side-product conversion (%)	
	TMP	3-MPA	<i>p</i> -TSA	(a)	(b)	(c)	(d)	(e)	$Y_1^a$	$Y_2^b$
preEXP-1	1.00	3.00	0.01	13.77	2.91	67.87	15.12	0.33	16.66	18.36
preEXP-2	1.00	3.30	0.01	10.83	2.54	69.40	16.76	0.47	13.37	19.77
preEXP-3	1.00	3.00	0.05	5.21	2.21	58.74	32.06	1.77	7.42	36.04
preEXP-4	1.00	3.30	0.05	6.28	4.90	52.36	34.27	2.19	11.18	41.36

<sup>a</sup>  $Y_1 = (a) \text{ peak area} + (b) \text{ peak area}$ . <sup>b</sup>  $Y_2 = (b) \text{ peak area} + (d) \text{ peak area} + (e) \text{ peak area}$ .



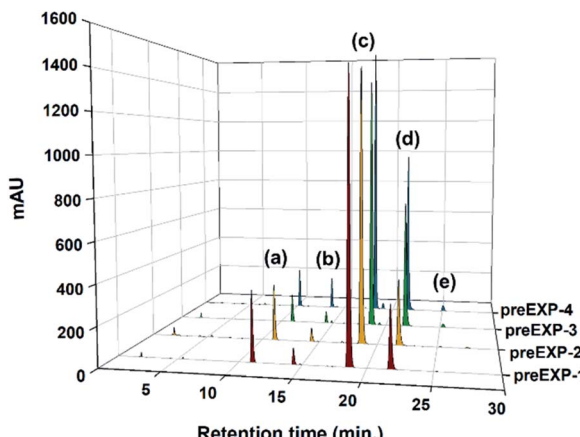


Fig. 2 HPLC chromatograms of crude product samples realized through the direct esterification preliminary reactions (entry preEXP-1–preEXP-4).

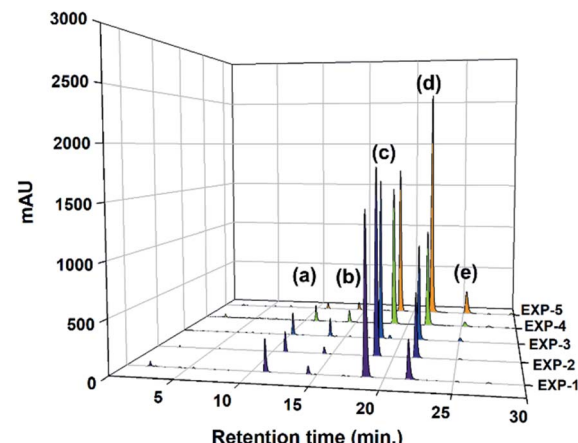


Fig. 3 HPLC chromatograms of product samples realized through direct esterification reactions (entry EXP-1–EXP-5).

of TMPMP, Y1, and Y2 side-products. As can be observed from Fig. 4, when the initial catalyst concentration increased from 0.01 to 0.03 mol mol<sup>-1</sup> of a TMP, a slight drop in desired TMPMP conversion was observed. The desired TMPMP conversion was quite a lot decreased when a higher catalyst concentration was employed. This effect was substantial, and the desired TMPMP conversion decreased from 69.41% to 35.94% when the catalyst concentration increased from 0.01 to 0.10 mol mol<sup>-1</sup> of a TMP.

A similar result has also been observed in Y1 side-product conversion with an increase in the catalyst concentration. However, the Y2 side-product conversion was increased. These results could indicate that the higher catalyst concentration could induce the thioesterification reaction since equilibrium in the reactions of carboxylic acids with thiols is not favorable for thioester formation under normal conditions, which means that a large activation barrier exists between the reactants (carboxylic acids and thiols) and the products (thioesters).<sup>19</sup>

The curing reaction of the synthesized TMPMP curing agent for DGEBA-type epoxy resin was assessed through the DSC technique. Their DSC thermograms were represented in Fig. 5 depending on TMPMP curing agents containing a different purity. The curing characteristics, including the curing onset temperature ( $T_i$ ), the exothermic maximum peak temperature

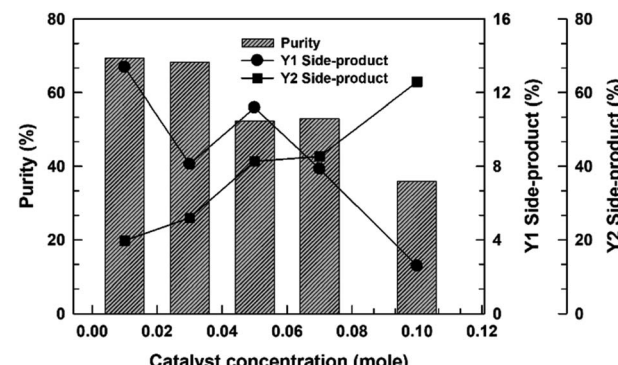


Fig. 4 The purities and side-product conversion for direct esterification reactions relying on the catalyst concentration.

( $T_p$ ), and the total curing reaction enthalpy are tabulated in Table 3. Furthermore, the gel-time for the thiol–epoxy curing systems containing 2,4,6-tris(dimethylaminomethyl) phenol as amine curing catalyst was monitored by a digital temperature recording device equipped with a temperature sensor. The temperature change during the curing reaction of the mixture was estimated at 30 s intervals for 90 min and the maximum temperature and the time to reach the maximum temperature

Table 2 The composition of the direct esterification reaction, a summary of the chromatographic analysis after the reaction, and SH values of the crude products

Entry	Reactant composition (mole)			Peak area integral (%)					Side-product conversion (%)		SH value (g eq <sup>-1</sup> )
	TMP	3-MPA	p-TSA	(a)	(b)	(c)	(d)	(e)	Y1 <sup>a</sup>	Y2 <sup>b</sup>	
EXP-1	1.00	3.30	0.01	10.83	2.54	69.41	16.76	0.47	13.37	19.77	131
EXP-2			0.03	5.85	2.27	68.20	22.73	0.95	8.12	25.95	129
EXP-3			0.05	6.28	4.90	52.36	34.27	2.19	11.18	41.36	132
EXP-4			0.07	4.44	3.42	52.89	36.21	3.03	7.86	42.66	132
EXP-5			0.10	1.18	1.40	35.94	53.81	7.66	2.58	62.87	132

<sup>a</sup> Y1 = (a) peak area + (b) peak area. <sup>b</sup> Y2 = (b) peak area + (d) peak area + (e) peak area.



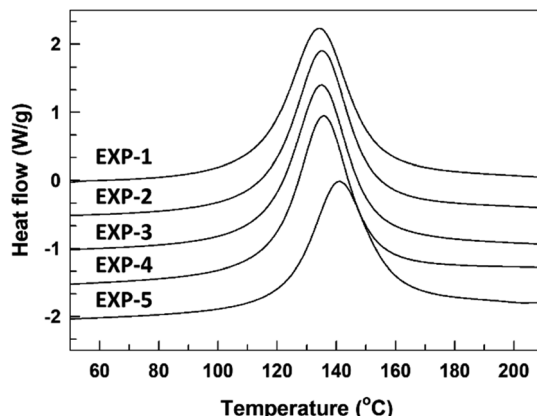


Fig. 5 DSC thermograms corresponding to dynamic curing for epoxy-TMPMP curing system relying on TMPMP purity.

were represented in Table 3. The time ( $T_{\text{gel}}$ ), on attaining the maximum temperature was determined as the gel-time (ESI: Fig. S5†). As indicated in Fig. 5, the exothermic peaks on the DSC thermograms mean that the curing reaction between the oxirane ring and the thiol group of TMPMP curing agents could occur. From these exothermic peaks, the reactivity of the TMPMP curing agent toward the epoxy resin could be analyzed from the onset temperature of the exothermic peak. The curing onset temperature of the epoxy-TMPMP curing system was slightly shifted to a higher temperature with increasing Y2 side-product in TMPMP curing agent. Decreasing the reactivity of the TMPMP curing agent could be associated with a plasticizing effect of the curing agent, which has a longer aliphatic chain due to thioester linkage.<sup>14</sup> Also, the single exothermic peak pattern during crosslinking with epoxy-TMPMP curing system could reflect that curing reaction involves the thiol–epoxy click reaction<sup>20</sup> and all the reactive components, which are in the stoichiometric ratio are taken up in the reaction.

From DSC thermograms, the thermal analysis for the cured epoxy resin is simple and essential to understand its molecular architecture. The DSC thermogram for base-catalyzed TMPMP-cured epoxy samples is presented in Fig. 6. The observed single  $T_{\text{g}}$ s indicated continuous phase morphology for the cured epoxy samples.<sup>21</sup> As we can see in Fig. 6, on increasing the Y2 side-product in the TMPMP curing agent,  $T_{\text{g}}$  value decreases. These results can be described by the increased flexibility of

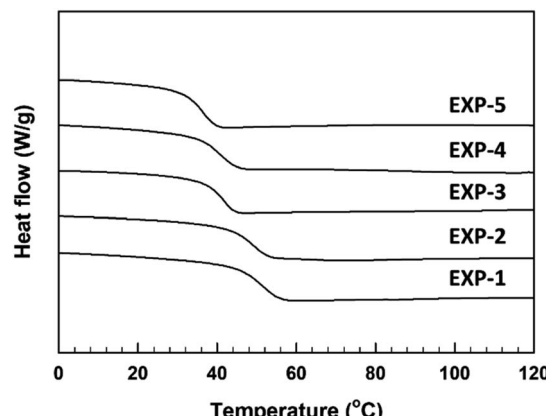


Fig. 6 DSC thermograms for base-catalyzed TMPMP-cured epoxy resin relying on TMPMP purity.

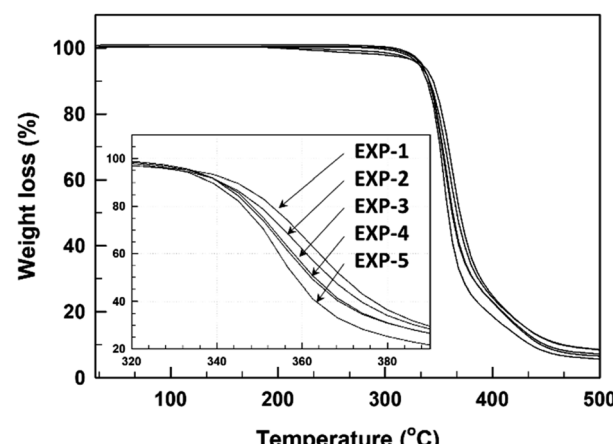


Fig. 7 TGA thermogram curves for base-catalyzed TMPMP-cured epoxy resin relying on TMPMP purity.

cured epoxy samples generated by thioester linkage in the crosslinked matrix. Introducing the relatively long-chain structure containing the thioester linkage in synthesized TMPMP results in cured epoxy resins with lower crosslink density, and consequently, lowering the  $T_{\text{g}}$  of the epoxy resin.

The thermal stability of the base-catalyzed TMPMP-cured epoxy resin was determined by thermogravimetry in an inert atmosphere, and their degradation curves are demonstrated in Fig. 7. The most relevant degradation parameters are summarized also in Table 3. Although there is not much noticeable difference among the thermal stability of these cured epoxy resins with TMPMP, the degradation temperature (20 wt% weight loss) is slightly decrease with increase Y2 side-product of TMPMP curing agent. This result could suggest that presence of thioester linkage in curing formulation did not significantly change the thermal stability of the cured epoxy resin.

Table 3 The curing behavior of epoxy-TMPMP curing system and thermal characteristics for base-catalyzed TMPMP-cured epoxy resins

Entry	Curing behavior		Thermal characteristics			
	$T_i$ (°C)	$T_p$ (°C)	$\Delta H$ (J g <sup>-1</sup> )	$T_{\text{gel}}$ (min)	$T_g$ (°C)	$T_d^a$ (°C)
EXP-1	113.4	134.5	413.5	26.4	49.1	353.1
EXP-2	115.6	135.5	426.9	30.6	47.5	350.1
EXP-3	116.1	135.4	388.1	32.5	39.6	348.4
EXP-4	118.0	136.1	380.0	37.9	39.1	347.6
EXP-5	122.5	141.4	326.9	58.5	34.1	340.5

<sup>a</sup> Measured at 20 wt% loss.

## Conclusions

The acid catalyst concentration was confirmed as one of the necessary synthesis parameters for the direct esterification



reaction between 3-mercaptopropionic acid (3-MPA) and trimethylolpropane (TMP). With the increase in the acid catalyst concentration of this esterification reaction, the purity of desired TMPMP was decreased whereas the production of thioester-based side-product was increased. The optimized catalyst concentration, which generated the minimum conversion of side-products ( $Y_1$  and  $Y_2$ ) was  $0.03 \text{ mol mol}^{-1}$  of a TMP and the desired TMPMP purity was 68.2%.

Higher purity of TMPMP curing agent exhibited a higher reactivity for thiol-epoxy click reaction. The  $Y_2$  side-product incorporating a thioester linkage within the TMPMP will express a plasticizing effect resulting in a less rigid network with a lower glass-transition temperature. According to these findings, their mechanical properties will be strongly reliant on the purity of TMPMP curing agent with a minimum portion of  $Y_2$  side-product.

## Experimental

### Materials

3-Mercaptopropionic acid (3-MPA), trimethylolpropane (TMP), *p*-toluenesulfonic acid (*p*-TSA), and 2,4,6-tris(dimethylaminomethyl)phenol were purchased from Sigma-Aldrich (Milwaukee, WI, USA) and were used without further purification. The diglycidyl ether of bisphenol A (DGEBA) epoxy resin (EEW = 185 g eq<sup>-1</sup>) was supplied by Shin-A T&C (Seoul, Korea). Other organic solvents and chemicals were purchased from SAMCHUN Chemicals (Seoul, Korea).

### General esterification experiments

Direct esterification reaction between 3-MPA and TMP is catalyzed by the *p*-TSA on a batch-type experimental system, where a 1000 mL three-necked round-bottomed flask is equipped with Dean-Stark trap and condenser for toluene reflux under inert atmosphere. 3-MPA, TMP, and *p*-TSA were sequentially added into the flask containing 250 mL of toluene and the mixture was refluxed throughout esterification reaction for 3–5 h. Upon accomplishment, the mixture was allowed to cool down to room temperature and then added 250 mL of toluene to dilute them. The mixture was transferred to a separating funnel to neutralize by adding the aqueous NaOH solution (10%). The organic phase layer, which mainly comprised of products, was later washed with distilled H<sub>2</sub>O three times to remove impurities, and subsequently dried with anhydrous magnesium sulfate. The solvent was evaporated, and the crude product was obtained after drying in vacuum oven for 2 days.

### Determination of SH value for synthesized mercaptoesters

After adding 0.1 g of mercaptoester sample in a beaker, 25 mL of chloroform was added and stirred for 10 minutes, then 10 mL of MeOH was added and stirred again for 10 minutes. The solution was titrated using a 0.1 N iodine standard solution with determining the end point is color of titrated solution change colorless to yellow. The SH value (g eq<sup>-1</sup>) was calculated by the following equation.

$$\text{SH value (g eq}^{-1}\text{)} = \frac{\text{sample weight (g)}}{0.1 \times 0.1 \text{ N iodine consumed (L)}}$$

### Preparation of curing mixture and cured samples

The mixtures were prepared by mixing stoichiometric proportions (1 : 1 eq/eq) of epoxide and thiol. For DSC experiments, a mixture of epoxy resin with TMPMP curing agent was prepared without basic catalyst. In base catalyzed formulations to analyze thermal behavior of cured epoxy samples, 2 phr of amine catalyst (parts of catalyst per hundred part of epoxy resin) was added after homogenization of epoxy-thiol mixture.

### Instruments

Nuclear magnetic resonance (NMR) for chemical structure analysis was performed on a JNM-LA400 (Jeol, Japan), using chloroform-*d*<sub>1</sub> (CDCl<sub>3</sub>) as a solvent. FT-IR spectra were recorded on a Nicolet iS10 spectrophotometer (Thermo Scientific Co., USA). LC-mass spectra were recorded on a LCMS-2020 spectrometer equipped with Shim-pack FC-ODS column (Shimadzu, Japan) under acetonitrile and water as the eluent and the gradient was from 40% of acetonitrile at 0 min to 70% of acetonitrile at 20 min. The purity characterization was performed on Agilent 1220 Infinity HPLC system equipped with Zorbax C18 column (Agilent, USA) under acetonitrile and aq. KH<sub>2</sub>PO<sub>4</sub> (0.01 mol) as the eluent and the gradient was from 40% of acetonitrile at 0 min to 70% of acetonitrile at 18 min. Differential scanning calorimetry (DSC) was carried out using a DSC 1 apparatus (Mettler Toledo, Ohio, USA) to characterize the thermal behavior of the samples. The scans were performed at a heating rate of 10 °C min<sup>-1</sup> under a N<sub>2</sub> gas atmosphere. Thermogravimetric analysis (TGA) measurements were performed on a Mettler TGA/SDTA 851e thermobalance from 30 to 600 °C with a heating rate of 20 °C min<sup>-1</sup> under a N<sub>2</sub> gas atmosphere.

### Author contributions

S.-M. Hong and S.-H. Hwang designed the experiments and wrote the manuscript. S.-M. Hong and O. Y. Kim synthesized and characterized the esterification reactions. S.-H. Hwang supervised the study. All of the authors discussed the results and commented on the manuscript.

### Conflicts of interest

There are no conflicts to declare.

### Acknowledgements

This work was supported by the GRRC program of Gyeonggi Province (GRRC Dankook 2016-B01).

### Notes and references

- 1 A. R. Jennings and D. Y. Son, *Chem. Commun.*, 2013, **49**, 3467–3469.
- 2 J. Hwang, D. G. Lee, H. Yeo, J. Rao, Z. Zhu, J. Shin, K. Jeong, S. Kim, H. W. Jung and A. Khan, *J. Am. Chem. Soc.*, 2018, **140**, 6700–6709.



3 N. Zivic, P. K. Kuroishi, F. Dumur, D. Gigmes, A. P. Dove and H. Sardon, *Angew. Chem., Int. Ed.*, 2019, **58**, 10410–10422.

4 I. Gadwal, J. Rao, J. Baettig and A. Khan, *Macromolecules*, 2014, **47**, 35–40.

5 C. T. Huynh, F. Liu, Y. Cheng, K. A. Coughlin and E. Alsberg, *ACS Appl. Mater. Interfaces*, 2018, **10**, 25936–25942.

6 I. Gadwal, M. C. Stuparu and A. Khan, *Polym. Chem.*, 2015, **6**, 1393–1404.

7 S. De and A. Khan, *Chem. Commun.*, 2012, **48**, 3130–3132.

8 N. Cengiz, J. Rao, A. Sanyal and A. Khan, *Chem. Commun.*, 2013, **49**, 11191–11193.

9 J. A. Carioscia, J. W. Stansbury and C. N. Bowman, *Polymer*, 2007, **48**, 1526–1532.

10 A. Brändle and A. Khan, *Polym. Chem.*, 2012, **3**, 3224–3227.

11 X. Yang, Y. Guo, X. Luo, N. Zheng, T. Ma, J. Tan, C. Li, Q. Zhang and J. Gu, *Compos. Sci. Technol.*, 2018, **164**, 59–64.

12 G. Ellson, M. Di Prima, T. Ware, X. Tang and W. Voit, *Smart Mater. Struct.*, 2015, **24**, 055001.

13 I. Isarn, X. Ramis, F. Ferrando and A. Serra, *Polymers*, 2018, **10**, 277.

14 A. Lungu, J. Ghitman, A. I. Cernencu, A. Serafim, N. M. Florea, E. Vasile and H. Iovu, *Polymer*, 2018, **145**, 324–333.

15 D. Guzmán, X. Ramis, X. Fernández-Francos and A. Serra, *Eur. Polym. J.*, 2014, **59**, 377–386.

16 J. Houk and G. M. Whitesides, *J. Am. Chem. Soc.*, 1987, **109**, 6825–6836.

17 S. Iimura, K. Manabe and S. Kobayashi, *Chem. Commun.*, 2002, 94–95.

18 B. M. Trost, *Science*, 1991, **254**, 1471–1477.

19 T. C. Bruice, in *Organic Sulphur Compounds*, ed. N. Kharasch, Pergamon, London, 1961, vol. 1, p. 421.

20 K. Strzelec, E. Lesniak and G. Janowska, *Polym. Int.*, 2005, **54**, 1337–1344.

21 K. Strzelec, N. Baczek, S. Ostrowska, K. Wasikowska, M. I. Szynkowska and J. Grams, *C. R. Chim.*, 2012, **15**, 1065–1071.

